Energy & Environmental Science

ROYAL SOCIETY OF CHEMISTRY

PERSPECTIVE

View Article Online
View Journal | View Issue

Cite this: *Energy Environ. Sci.*, 2020, **13**, 1694

The relative insignificance of advanced materials in enhancing the energy efficiency of desalination technologies†

Sohum K. Patel, ‡[ab] Cody L. Ritt, ‡[a] Akshay Deshmukh,[a] Zhangxin Wang,[a] Mohan Qin,[ab] Razi Epsztein[a] and Menachem Elimelech *[ab]

As the threat of global water scarcity continues to grow, a myriad of scientific effort is directed towards advancing water desalination technologies. Reverse osmosis (RO), solar thermal desalination (STD), and capacitive deionization (CDI), have dominated recent pressure-, thermal-, and electro-driven desalination research efforts, respectively. Despite being based on distinctive driving forces and separation mechanisms, research of these three processes has primarily shared the same fundamental goal and approach: the minimization of energy consumption for desalination through the development of novel materials. A variety of materials have been studied and proposed to enhance RO membrane permeability, STD solar absorptivity, and CDI electrode capacitance. Here, we critically discuss the advanced materials investigated and assess their efficacy in augmenting the energy efficiency of desalination. Through our systematic analysis, we show that materials have relatively insignificant impact on further increasing energy efficiency, regardless of the process applied. We provide insights into the inherent limitations of advanced materials for improving the energy efficiency of each of the evaluated technologies and propose more effective materials-based research directions. We conclude by highlighting the opportunity for considerable improvement in energy efficiency *via* system design, reinforcing the critical need for a paradigm shift in desalination research.

Received 3rd February 2020,
Accepted 6th April 2020

DOI: 10.1039/d0ee00341g

rsc.li/ees

Broader context

The progression of global water scarcity continues to promote intensive research on desalination—a process involving the separation of salt from saline waters. As with any separation, desalination inherently requires the input of energy. Minimization of the required energy (or maximization of energy efficiency) has long remained the primary objective of desalination research efforts. With several distinct technologies for desalination having been developed, recent efforts have overwhelmingly focused on the innovation and application of novel materials to optimize the performance of existing technologies. In this perspective, we critically assess this ongoing research direction by systematically evaluating the role and potential of advanced materials in enhancing the energy efficiency of desalination. By extending our analysis to technologies representative of each desalination mechanism—pressure-, thermal-, and electro-driven—we broadly demonstrate the severely limited potential of materials in further reducing the energetic demand of desalination. Our findings highlight that consequential and sustained advancements in the field of desalination will require an overhauled approach.

Introduction

Already affecting over two-thirds of the world population and continuing to expand, global water scarcity poses as one of the greatest threats to the sustained development of humanity. With population growth, industrialization, and climate change driving the pollution and depletion of the planet's severely limited freshwater resources, the need to harness unconventional water sources is paramount.[1] However, these sources, such as seawater and brackish groundwater, are generally characterized by high salinities, requiring the removal of salt—through a process known as desalination—for effective utilization. In light of the growing concerns of water scarcity, desalination capacity has more than tripled in the past two decades.[2] Nonetheless, desalination, like all separation processes, requires the input of energy. Hence, as global reliance on alternative water sources increases,

[a] *Department of Chemical and Environmental Engineering, Yale University, P.O. Box 208268, New Haven, Connecticut 06520, USA. E-mail: menachem.elimelech@yale.edu; Fax: +1-203-432-2881; Tel: +1-203-432-2789*

[b] *Nanosystems Engineering Research Center for Nanotechnology-Enabled Water Treatment (NEWT), Yale University, New Haven, Connecticut 06520, USA*

† Electronic supplementary information (ESI) available. See DOI: 10.1039/d0ee00341g

‡ These authors contributed equally to this work.

it is essential to minimize the energy consumption of desalination to ensure a sustainable, water-secure future.

Developments in the field of desalination have culminated in several distinct technologies, which can broadly be classified according to the driving force used to facilitate the salt-water separation. Most desalination processes rely on either pressure-, thermal-, or electrical-based chemical potential gradients to induce salt removal. Reverse osmosis (RO)—currently the most widely employed and energy efficient desalination technology—is pressure-driven, utilizing a semipermeable membrane for the selective passage of water molecules over salt ions.[3–5] To drive water through the membrane and produce purified water, RO requires the application of hydraulic pressure in excess of the osmotic pressure of the generated brine. Current RO membranes and membrane modules, however, lack the mechanical robustness required to overcome the osmotic pressures encountered during the treatment of hypersaline solutions.[6] Thermal-driven technologies have thus withheld applications in the desalination of brines, despite being inherently energy intensive due to the required vapor–liquid phase changes. To offset the large latent heat of vaporization, recent thermal-driven efforts have shifted towards the use of renewable energy sources—particularly solar. The optimization of solar thermal desalination (STD) systems and the application of solar-based heating for membrane distillation (MD) have become prominent areas of investigation.[7–9] In contrast to thermal-driven processes, electro-driven technologies are most practical in the desalination of brackish and low-salinity waters, with the advantage of circumventing the use of high pressures or temperatures. Capacitive deionization (CDI), founded on the principle of storing salt ions in electrodes, has experienced a surge in research efforts, becoming the most investigated electro-driven desalination technology over recent years.[10,11]

Regardless of the mechanism, energy consumption remains a chief concern and area of investigation of desalination processes.[4] To assess the current state and future potential of desalination technologies, it is necessary to define the minimum

Sohum K. Patel

Sohum Patel is a PhD student working with the Elimelech Research Group in the Department of Chemical and Environmental Engineering at Yale University. He received his BSc in Chemical Engineering from the University of Illinois at Urbana-Champaign. Sohum's research is broadly focused on the development of water treatment and desalination technologies, with specific emphasis on electro-driven processes. He is particularly interested in understanding and enabling enhanced ion–ion selectivity to address current challenges at the water–energy nexus and to facilitate resource recovery.

Cody L. Ritt

Cody Ritt is a PhD candidate in the Department of Chemical and Environmental Engineering at Yale University. Prior to Yale, he received his BSc and MSc in Civil Engineering at North Dakota State University. He is interested in understanding fundamental transport processes at the water–energy nexus, and his research activities focus on bridging knowledge gaps surrounding nanoconfined transport by employing solid-state devices as model nanofluidic systems.

Akshay Deshmukh

Akshay Deshmukh is a postdoctoral associate in the Department of Mechanical Engineering at the Massachusetts Institute of Technology working on the thermodynamic modeling of aqueous–organic-electrolyte mixtures and membrane-based organic solvent separations. He received his PhD in Chemical and Environmental Engineering from Yale University where his research focused on driving theory-guided membrane design through heat and mass transport modeling. Prior to Yale, he completed his BA and MEng in Chemical Engineering at the University of Cambridge.

Zhangxin Wang

Zhangxin Wang is a postdoctoral associate working with Prof. Menachem Elimelech in the Department of Chemical and Environmental Engineering at Yale University. He received his BSc from Xi'an Jiaotong University, MSc from Purdue University, and PhD from Vanderbilt University in Environmental Engineering. His research interests focus on addressing the challenges at the water–food–energy nexus using membrane technologies. He is also interested in the development of novel membranes for water purification and wastewater treatment.

specific energy requirement of desalination (SE_{min}). The SE_{min} is representative of a thermodynamically reversible process and is thereby equivalent to the Gibbs free energy of separation.[12] However, all practical desalination processes suffer irreversible energy losses, causing the actual specific energy requirement (SE) to be greater than the ideal SE_{min}. Entropic losses associated with establishing finite driving force and separation kinetics are inevitable, while losses from parasitic mass-, charge-, and heat-transfer resistances theoretically have the potential to be reduced from improvements in material and process design.[13,14] For example, the advent of thin-film-composite (TFC) polyamide membranes and efficient energy recovery devices has substantially reduced the energetic demand of seawater RO, enabling current state-of-the-art systems to perform within two-fold of the thermodynamic minimum specific energy requirements.[4]

Research aimed at minimizing the energy consumption of desalination processes has increasingly followed a materials-based approach. RO, STD, and CDI, have each targeted specific material properties, expecting substantial returns in process performance (Fig. 1). In RO, the demonstration of significant flow enhancement across the smooth graphitic planes of various carbon nanomaterials has led researchers to pursue highly permeable RO membranes which could overcome the constraint of the TFC permeability–selectivity trade-off. Work in solar thermal desalination (STD) continues to introduce novel solar absorber materials to improve the efficiency of vapor generation from solar energy.[15,16] Ongoing CDI materials research has targeted high capacitance electrodes, largely through the incorporation of carbon nanomaterials and ion-intercalation compounds.[17] Nonetheless, the effectiveness of these research avenues on reducing the energy consumption of desalination remains unclear and largely unexplored.

With research in the field of desalination increasingly relying on the innovation of novel materials, careful assessment of this approach is crucial. In this perspective, we aim to systematically evaluate the role and potential of advanced materials in enhancing the energy efficiency of desalination. We encompass each of the three major classes of desalination by performing in depth analysis of advanced materials for RO, STD, and CDI. For each technology, we first expand on the rationale which has led to targeting particular material properties. Next, we assess the efficacy of developed materials on reducing energy consumption, revealing the highly consequential finding that advanced materials offer little opportunity for further enhancement of desalination energy efficiency. We provide insight into the fundamental limitations which constrain energetic performance and suggest the redirection of materials research to more impactful applications extending beyond the enhancement of energy efficiency. We conclude by emphasizing the comparatively large potential for improvements in desalination energy efficiency through system design.

Pressure-driven desalination: reverse osmosis

Reverse osmosis (RO), a pressure-driven membrane-based process, is at the forefront of advanced water treatment technologies, accounting for 72% of the global desalination capacity.[2] This commanding market share is largely due to the high energy efficiency of RO, which was achieved through the advent of highly permeable and water–salt selective thin-film composite (TFC) polyamide membranes, introduction of energy recovery devices to recoup the energy of the pressurized brine, and use of highly-efficient pumps.[4] Pressure-driven membrane processes operate by the application of a hydraulic pressure (ΔP) greater than the transmembrane osmotic pressure difference ($\Delta\pi_m$), driving a water flux (J_w) from the high salinity feed to the low salinity permeate. Due to the dense, nonporous nature of polyamide films, water flux across the membrane can be described by the solution-diffusion model, $J_w = A(\Delta P - \Delta\pi_m)$,[18] where A is the water permeability coefficient. Similarly, salt flux (J_s) is modeled as Fickian diffusion $J_s = B(\Delta C_m)$, where B is the salt permeability

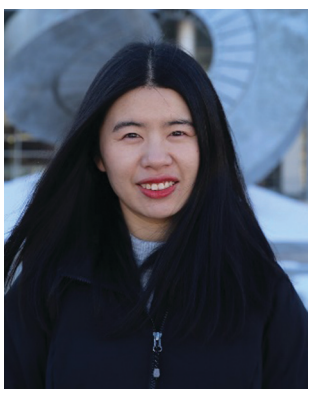

Mohan Qin

Mohan Qin is an assistant professor in the Department of Civil and Environmental Engineering at University of Wisconsin–Madison. She received her BS from Shandong University, MS from Peking University, PhD from Virginia Tech, and postdoctoral training from Yale University. Her research interests include the development of novel approaches for resource recovery from wastewater and selective ion removal from brackish water.

Menachem Elimelech

Menachem Elimelech is the Roberto Goizueta Professor at the Department of Chemical and Environmental Engineering at Yale University. His research interests include emerging membrane-based technologies at the water–energy nexus, materials for next generation desalination and water purification membranes, and environmental applications of nanomaterials. Professor Elimelech is a Clarivate Analytics (formerly Thomson Reuters) Highly Cited Researcher in two categories: chemistry and environment/ecology. He is a member of the US National Academy of Engineering and a foreign member of the Chinese Academy of Engineering.

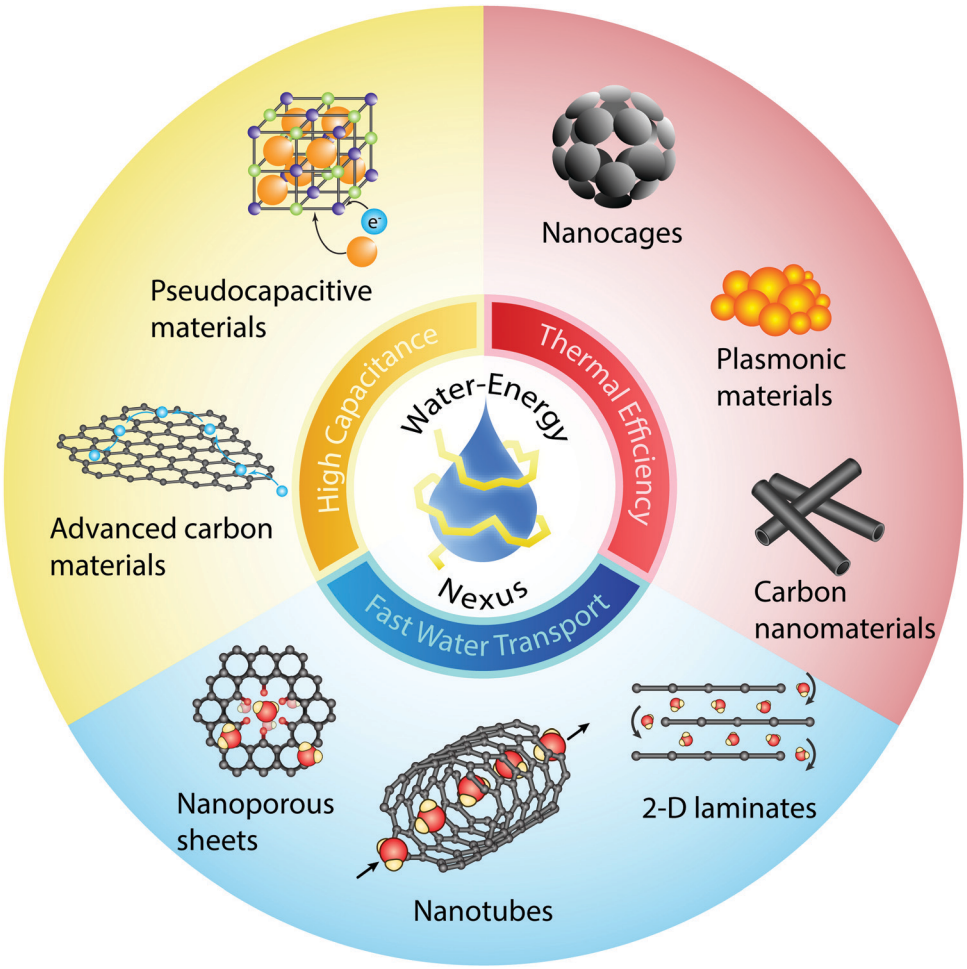

Fig. 1 Examples of novel materials, and their respective properties, proposed to enhance the energy efficiency of desalination processes. Fast water transport, increased solar absorptivity, and ultra-high capacitance or increased electrical conductivity are several properties that have been highly targeted to increase energy efficiency in pressure-, thermal-, and electro-driven desalination processes, respectively.

coefficient and ΔC_m is the concentration difference across the membrane active layer. Water–salt selectivity, represented by the ratio of the water and salt permeability coefficients, stems from increased steric resistance to salt partitioning into and diffusing between molecular voids throughout the membrane active layer.[18]

Although the development of TFC polyamide membranes represented a breakthrough for desalination, inherent material limitations have constrained further improvements in performance over the past decade.[4] Like other separation materials, desalination membranes exhibit a permeability–selectivity tradeoff;[18] hence, the water–solute selectivities achievable within the range of operationally-feasible water permeabilities ($\sim$1–3 L m^{-2} h^{-1} bar^{-1}) are limited.[19] In an effort to overcome the limitations imposed by the permeability–selectivity tradeoff, substantial research efforts have proposed the use of novel materials, such as one-dimensional (1-D) nanotubes, two-dimensional (2-D) nanosheets, and biological channels. These novel materials have been lauded for their ultra-high water permeability, high water–solute selectivity, and tunability—desirable characteristics for next-generation desalination membranes.[20]

With permeabilities of novel-material membranes projected to surpass current TFC membranes by two to three orders of magnitude,[21] the prospect of improved desalination energy efficiency from ultra-permeable systems has sparked considerable interest in the membrane community.[22,23] Ultra-fast water transport through novel material channels results from flow enhancement under slip flow conditions.[24] Slip flow occurs when the interactions between water molecules and the channel surface result in a nonzero velocity, leading to a breakdown of the commonly assumed no-slip boundary condition. This case often arises when considering atomically smooth, hydrophobic surfaces, such as graphitic planes.[25] However, its relevance to fluid flow is only observed when the slip length is of similar magnitude to the channel size through which flow is occurring. Further, the exceptionally small scale of novel material channels—as small as 3 Å in aquaporin Z[26]—can lead to slip lengths several orders of magnitude larger than the channel size.[27] The mechanism behind such immense slip enhancement is surmised to result from the increased structural order of water molecules subjected to extreme confinement.[28]

The relationship between channel properties, slip flow, and water permeability is depicted in Fig. 2a. Channel permeability can

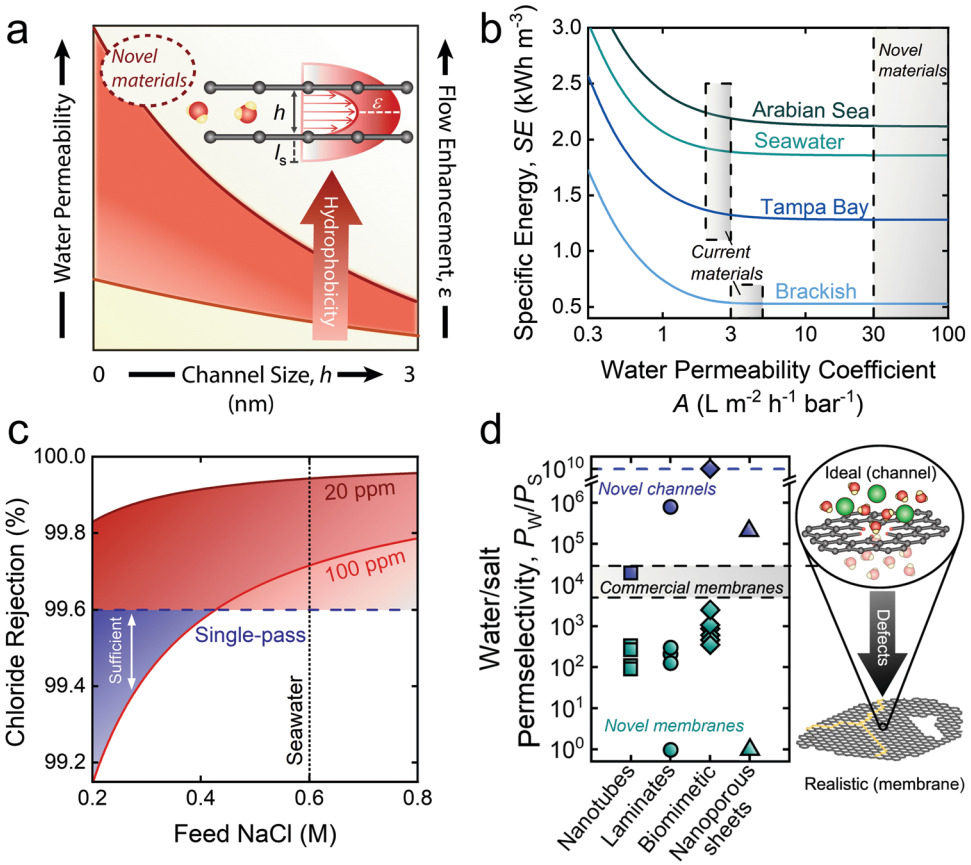

Fig. 2 The role of enhanced permeability and water–salt selectivity in advancing pressure-driven desalination processes. (a) Schematic of slip flow and its relation with water permeability. Slip length (l_s), representing an increase in the flow velocity profile beyond the channel surface, enhances the total flow through the channel, resulting in increased water permeability. The red shaded band roughly illustrates the roles of channel hydrophobicity and size on water permeability. Smaller channels generally experience higher flow enhancement due to ordered structuring of water—an effect that can be accentuated with a reduction in the frictional drag experienced by water molecules *via* increased channel hydrophobicity. (b) Specific energy (SE) requirements for the desalination of saline feedwaters from the Arabian Sea, typical seawater, Tampa Bay, and brackish groundwater with respect to membrane water permeability. SE was modeled at operationally relevant water recoveries: 75%, 50%, 50%, and 40% for brackish water (5.8 g L^{-1}), Tampa Bay (25 g L^{-1}), seawater (35 g L^{-1}), and the Arabian Sea (45 g L^{-1}), respectively. (c) Chloride rejections required to meet permeate standards of 100 and 20 ppm chloride for use in irrigation in Israel. (d) Water/salt selectivity (P_W/P_S) attained by novel channels, novel membranes, and commercial membranes. Although novel channels have shown promise for ultra-high selectivity experimentally (represented by points)[38–41] and theoretically (represented by dashed blue line), framework defects induced by fabrication techniques has hindered the selectivity of novel membranes. The blue dashed line is a proxy for complete salt exclusion. Novel materials assessed were nanotubes,[139–142] 2-D laminates,[29,143–148] biomimetic channels,[149–154] and nanoporous sheets.[155,156]

be expressed in terms of slip flow by solving the Navier–Stokes equation:[29]

$$\hat{P}_W = \frac{h^2}{8\eta}\left[\left(1+\frac{2l_s}{h}\right)^2 - \frac{1}{3}\right] \quad (1)$$

where $\hat{P}_W$ is the intrinsic water permeability of the channel, η is the viscosity of water, l_s is the slip length, and h is the channel size. Though theoretical simulations have failed to successfully predict the results of experimental measurements,[24] the potential for ultra-high permeabilities has spearheaded research efforts in the development of novel materials for next-generation desalination membranes.

Despite being exciting in concept, the practical implications of ultra-permeable membranes toward increased energy efficiency in RO desalination are minimal. Rigorous process-scale modeling has revealed that increasing membrane permeability above the values of current commercial TFC membranes offers little opportunity for reducing specific energy consumption (SE) in seawater RO (SWRO).[19,30] In Fig. 2b, we extend the modeling from these studies, showing the specific energy requirements of desalination for permeability coefficients up to 100 L m^{-2} h^{-1} bar^{-1} with varying feedwater salinities and water recoveries (WR): Arabian Sea (45 g L^{-1}, WR = 40%), typical seawater (35 g L^{-1}, WR = 50%), Tampa Bay, Florida (25 g L^{-1}, WR = 50%), and brackish water (5.8 g L^{-1}, WR = 75%). Water recoveries were based on typical operation for the different feed sources.

The results in Fig. 2b show that initial increases in the water permeability coefficient sharply decrease the SE. However, continued increase of the permeability leads to little reduction in SE for all feed salinities. Current TFC polyamide membranes are capable of operational membrane permeabilities in the

range of 2–3 L m^{-2} h^{-1} bar^{-1} for high feed salinities, and 3–5 L m^{-2} h^{-1} bar^{-1} for brackish waters (BWRO).[19] The lower ends of these permeability ranges result in an SE of 1.92 kW h m^{-3} for typical seawater (35 g L^{-1}) and 0.54 kW h m^{-3} for BWRO. When the permeability coefficient is increased to 100 L m^{-2} h^{-1} bar^{-1}, the SE of seawater and brackish water desalination decrease only by 3.4% and 1.4%, respectively, clearly highlighting the marginal role of ultra-permeable membranes in improving the energy efficiency of RO desalination. Furthermore, though ultra-permeable membranes would facilitate high water fluxes and theoretically reduce the required membrane area (or number of membrane modules),[30] intensified concentration polarization[19] and membrane fouling[31,32] would severely reduce the effective driving force, rendering operation at high water flux impractical.

Accordingly, we emphasize that ongoing efforts aimed at augmenting water permeability should be redirected to increasing membrane water–solute selectivity—an avenue with the potential to substantially improve the efficiency of RO.[19] Although current TFC membranes already possess high water–solute selectivity (NaCl rejection of 99.6 to 99.8%),[4] stringent regulations render these membranes inadequate for certain desalination applications. For instance, current TFC membranes cannot meet the $<$20 ppm chloride standard set forth by seawater desalination plants in Israel with a single pass configuration.[33] The use of desalinated seawater for irrigation, which is common in arid regions of Spain, also demands intense treatment, with chloride levels recommended below 3 meq L^{-1} ($\sim$100 ppm chloride) to avoid chloride-related plant toxicities.[34] We further highlight the need for increased selectivity by demonstrating the failure of current TFC membranes to meet these standards in a single pass for a wide range of feed salinities (Fig. 2c). Several other important applications also call for increased water–solute selectivity, such as boron removal in seawater desalination, micropollutant removal for potable reuse of wastewater, and high-purity water production.[19] Next-generation membranes with ultra-high rejection could obviate the need for extensive post-treatment steps, such as additional RO passes.

Theoretical and molecular simulations have revealed the potential for ultra-high water–solute selectivity through the use of nanotubes,[35] laminated nanosheets,[36] biomimetic channels,[37] and nanoporous sheets.[21] Experimental studies using isolated channels have also recently verified the remarkable selectivity of novel materials.[38–41] The highly selective and tunable nature of these novel materials offer advantages for a wide array of water treatment applications, making them primary candidates for the design of next-generation desalination membranes.[20] However, incorporation of these materials in membranes has been hindered by fabrication-induced defects within the separation layer and supporting substrate. Grain boundaries, tears, wrinkles, and framework defects in large-scale 2-D laminate and nanoporous sheet membranes present little resistance to solute transport, thus reducing the water–solute selectivity of the membrane.[29,42] The immobilization and alignment of novel materials, such as carbon nanotubes (CNTs) and aquaporins, also presents challenges. For example, immobilization of CNTs in support matrices has proven difficult, likely due to the lack of stabilizing interactions at the channel–matrix interface.[43]

We illustrate the detrimental effect of fabrication-induced defects in Fig. 2d, where the water–salt permselectivities of novel-material membranes are compared with their ideal counterparts (*i.e.*, well-defined channels). Permselectivities were calculated based on reported experimental details and measurements (see ESI† for details). Incorporation of novel materials into membrane matrices results in a precipitous drop (several orders of magnitude) in water–salt permselectivities, resulting in selectivities far below current TFC membranes. The limitations posed by fabrication-induced defects remain a critical limiting factor in the development of practical novel-material membranes. Overcoming these defects will require increasingly ordered systems with high levels of control over environmental conditions and material variability during fabrication. While currently achievable in small-scale experiments,[38–41] scale up for commercial use is a daunting task.

Despite substantial research efforts toward enhancing membrane permeabilities *via* material design, the resulting reduction in the energy consumption of RO has been minimal. Instead, we reiterate the critical need for increased water–solute selectivity to enhance desalination process efficiency. Novel materials can potentially improve water–salt selectivity, but their incorporation into membrane matrices currently remains hindered by the formation of defects during fabrication. The pervasiveness of defect formation during conventional fabrication necessitates significant advancement of synthesis techniques to develop highly selective novel-material membranes.

Thermal-driven desalination: solar thermal desalination

In thermal-driven desalination processes, fresh water is separated from non-volatile solutes by evaporation and subsequent condensation, with the required energy being strongly dependent on the latent heat of evaporation and the extent of heat recovery which can be achieved. The latent heat of water evaporation, being two orders of magnitude larger than the thermodynamic minimum specific energy of separation, makes thermal desalination technologies intrinsically energy intensive compared to pressure-driven desalination.[4,44] Nonetheless, thermal-driven desalination is needed for the desalination of hypersaline feedwaters as the osmotic pressure of such waters can far exceed the allowable working hydraulic pressure of pressure-driven desalination.[45,46] If powered by fossil fuels, the energy demand of thermal desalination technologies would prove unsustainable—incurring both high costs and adverse environmental impacts.[47]

In light of the high energy demand of thermal desalination technologies, solar-thermal desalination (STD), in which renewable solar energy is used to drive thermal desalination, has attracted increasing research attention in recent years.[48,49] While numerous STD systems and configurations have been proposed, most research efforts have been devoted to the development of efficient solar absorbers. Recent studies have also introduced solar-driven surface heating membrane distillation, an STD system in which the solar absorbers are directly incorporated into the thermal desalination process.[50,51]

The specific water productivity (SWP), defined as the volume of water produced per area of solar irradiation per time, is widely used as a quantitative metric for energy efficiency of an STD system.[15,16,52–54] Based on our recent study,[9] an STD process can be divided into two steps: (i) solar vapor generation and (ii) vapor to water production. The gain output ratio (GOR) is representative of the vapor to water production efficiency, while the solar vapor generation efficiency is defined as η_s. Hence, the SWP can be determined from[9]

$$\mathrm{SWP} = \frac{E}{L}\eta_s \mathrm{GOR} \quad (2)$$

where E is the given solar irradiance and L is the latent heat of water evaporation.

Most STD studies focus on improving vapor generation efficiency by developing advanced solar absorbers. Specifically, two material components of solar absorbers have been investigated extensively: (i) materials with ultra-high solar absorptivity (*e.g.*, carbon nanomaterials, plasmonic materials, and metal oxide nanomaterials),[15,16,55,56] and (ii) underlying porous supports made of low-thermal-conductivity materials (*e.g.*, foams and wood).[52,57] A solar absorber made of size-distributed plasmonic nanoparticles with an underlying porous foam support is shown in Fig. 3a as an example. The size-distributed nanoparticles effectively absorb solar energy due to localized surface plasmon resonance, resulting in ultra-high solar absorptivity (α).[15,16] Meanwhile, the porous foam support significantly reduces conductive heat loss to the underlying saline water, leading to high thermal efficiency for water evaporation (η_t).[53,57] With high α and η_t, the solar energy is efficiently converted to thermal energy that is used to generate water vapor. Hence, novel material-based solar absorbers can enhance the solar vapor generation efficiency ($\eta_s = \alpha\eta_t$),

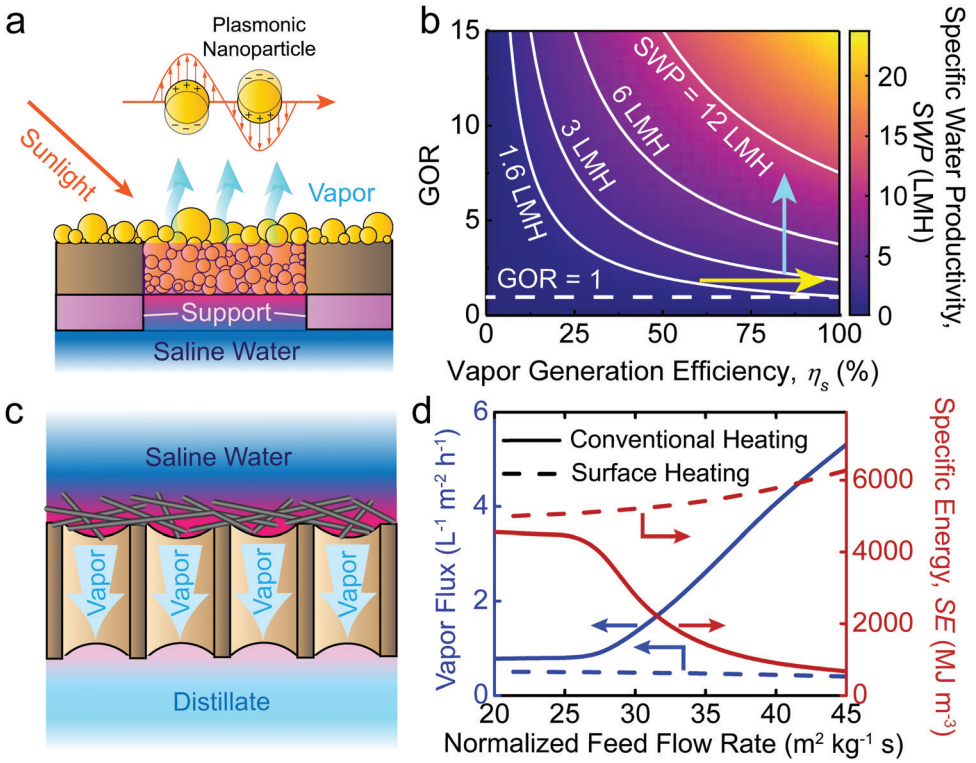

Fig. 3 The impact of novel materials on thermal desalination performance. (a) Schematic of a solar thermal desalination system (STD) equipped with a solar absorber based on plasmonic nanoparticles. The solar absorber is constructed by embedding size-distributed plasmonic nanoparticles on a porous substrate and placing a porous low-thermal-conductivity support underneath. An ultra-high solar absorptivity (0.99) can be achieved because of the localized surface plasmon resonance enabled by the nanoparticles. In addition, the porous low-thermal-conductivity support can effectively reduce the conductive heat loss to the saline water, thereby enhancing the thermal efficiency of vapor generation. (b) Specific water productivity (SWP) as a function of vapor generation efficiency (η_s) and GOR (parameter quantifying the efficiency of latent heat recovery) in STD systems. For the calculation, the solar irradiance is 1000 W m^{-2} (*i.e.*, one-sun illumination) and the latent heat of water evaporation is 2260 kJ L^{-1}. The solid white curves are the reference curves of different SWP, and the dashed white line denotes the performances of STD systems without latent heat recovery (*i.e.*, GOR = 1). The yellow arrow refers to increasing η_s *via* improved materials. The blue arrow represents the implementation of latent heat recovery measures. (c) Schematic of surface-heating membrane distillation (MD) enabled by carbon nanotube-coated MD membranes. The carbon nanotube-coated MD membranes can be surface heated by applying alternate current (Joule heating) or solar irradiance (photothermal heating) on the coating layer. Water vapor is produced and transported from the saline side to the distillate side due to the temperature-driven vapor pressure difference. (d) Vapor flux (left vertical axis, blue) and specific energy consumption (red vertical axis, red) as a function of normalized feed flow rate in conventional heating (solid curves) and surface heating (dashed curves) direct contact MD (DCMD) systems. The feed (hot) and distillate (cold) stream flow counter-currently with the same flow rate at the module inlets. The feed and distillate inlet temperatures, the heat input, and the membrane areas in the two systems were kept the same. For the surface heating DCMD, the heating source was assumed as one sun solar irradiance (*i.e.*, 1000 W m^{-2}). In the conventional heating DCMD, the minimum approach temperature in the heat exchanger was assumed to be 5 °C.

theoretically resulting in improvement of the overall energy efficiency of STD systems.[9]

In addition to η_s, GOR is another important parameter that influences SWP. GOR is defined as the kilograms of distilled water produced per kilogram of water vapor provided and quantifies the degree to which the latent heat of evaporation is reused in the system.[58] A high GOR is achieved when the latent heat of evaporation released during vapor condensation is reused to generate additional vapor for water production. The dependence of SWP on η_s and GOR is further illustrated in Fig. 3b. As shown, improvement of either η_s (yellow arrow) or GOR (blue arrow) can lead to an increase of SWP, indicating that the development of novel materials and the implementation of latent heat recovery can increase the energy efficiency of STD systems, albeit to different extents. To date, STD systems with materials having $\eta_s > 90\%$ have already been developed.[59,60] We consider the case in which further materials development of solar absorbers allows for ideal solar vapor generation efficiency to be achieved ($\eta_s > 100\%$). In the case of no latent heat recovery (GOR = 1), the maximum SWP under one sun solar irradiance (1000 W m^{-2}) increases from 1.4 L m^{-2} h^{-1} (η_s = 91.5%, an SWP demonstrated in the literature[59]) to $\sim$1.5 L m^{-2} h^{-1}—a marginal increase of only $\sim$10%. In contrast, if latent heat recovery is implemented, an SWP of over 3 L m^{-2} h^{-1} can readily be achieved with a GOR of 3 and conservative η_s of 75%. Accordingly, we emphasize that with the vapor generation efficiency of current solar absorber materials already approaching the theoretical limit,[9] enhancement of latent heat recovery is a substantially more rewarding direction for achieving higher energy efficiency (or SWP) in STD systems.

Mature thermal desalination technologies, such as multi-effect distillation (MED) and multistage flash (MSF), have undergone extensive optimization to effectively recover the latent heat of evaporation.[61,62] Hence, the incorporation of external solar thermal collectors with these technologies has produced STD systems with high GOR values.[63,64] High capital investments, however, typically limit MED and MSF to large production applications, making their STD systems unfeasible for modular or off-grid use. In recent years, small-scale STD systems with latent heat recovery have been proposed by using solar thermal collectors to drive membrane distillation (MD) systems.[9,65] Since the solar absorptivity of the solar thermal collectors can be very high (>90%),[66] the SWP of such STD systems mainly depends on the energy efficiency of the MD component.

MD is an emerging thermal desalination technology enabled by a microporous hydrophobic membrane, placed between a hot saline stream (feed) and a cold fresh water stream (distillate). The transmembrane vapor pressure gradient drives water vapor through the membrane into the distillate side—where condensation produces fresh water—while salt and non-volatiles are rejected by the membrane. Direct contact MD (DCMD) with countercurrent flow of feed and distillate streams is the simplest MD configuration to effectively utilize solar thermal collectors. In a DCMD-based STD system, the influent feedwater is preheated by the effluent distillate water using a heat exchanger, thereby recovering the latent heat of vapor condensation embedded in the distillate stream.[67,68] The temperature of the preheated feedwater is then further increased by a solar thermal collector to attain the operating temperatures required before entering the membrane module.

A modification of the DCMD configuration, which is presumed to reduce the energy consumption of the process, is the heating of the membrane surface—and the water within its direct vicinity—rather than the bulk feed solution. Surface heating intuitively offers the advantage of reducing the required energy since less water is heated, while also eliminating temperature polarization and its detrimental effects.[69,70] With surface-heating DCMD gaining considerable momentum, recent studies have proposed the use of solar energy by developing MD membranes with photothermal surface coatings (*e.g.*, plasmonic nanoparticles or carbon nanotubes), effectively introducing a novel STD system which obviates the need for external solar collectors.[50,51] While the benefits of surface heating are apparent for single-pass DCMD operation—common in small laboratory-scale systems—our recent process modeling importantly reveals that conventionally heated DCMD is in fact considerably more energy efficient under practical operation involving recirculation of the feed stream (see ESI† for details). In Fig. 3d we show the performance of conventionally heated and surface heated DCMD configurations operated with feed recirculation over a range of feed flow rates. Conventional heating demonstrates both significantly higher water vapor flux and lower specific energy consumption (SE). The large disparity in the efficiencies of the two processes is due to varying degrees of latent heat recovery. As previously described, the latent heat of water vapor condensation can be effectively recovered using a heat exchanger in conventional heating DCMD. However, in surface heating DCMD, it is very challenging to recover latent heat of water vapor condensation from the distillate stream because the temperature of the effluent distillate stream is similar to, or only slightly higher than the influent feed stream. With poor latent heat recovery (*i.e.*, small GOR), the specific energy (SE) for water production is large (*i.e.*, SE = *L*/GOR),[9] and given the same input energy (*i.e.*, solar irradiance in Fig. 3d), large SE results in low water vapor flux. In addition to photothermal MD membranes, electrically conductive MD membranes have also been fabricated to enable electro-driven surface heating DCMD systems (*i.e.*, Joule heating).[69] However, based on the above discussion, regardless of the power source applied, surface heating DCMD is unable to improve the energy efficiency of conventional heating DCMD.

Instead of developing advanced membranes to improve the energy efficiency of surface heating MD, we emphasize the urgent need for MD membranes with enhanced robustness. At present, MD is used to desalinate relatively 'clean' saline waters due to the high fouling and wetting propensity of current membranes.[71] In MD, membrane fouling largely occurs in the form of pore blockage by foulants (*e.g.*, natural organic matters and oil droplets), resulting in a substantially reduced water vapor flux.[72,73] Unlike fouling which is a challenge of all membrane processes, membrane wetting is a unique phenomenon in MD, in which saline feed solution penetrates through the hydrophobic MD membrane, leading to process failure.[74,75] Membrane wetting typically occurs in the presence of contaminants

which lower the surface tension of the feed solution (*e.g.*, surfactants).[75,76] To mitigate MD membrane fouling and wetting, novel membranes with special wettability have been proposed.[77] These include (i) composite MD membranes with a superhydrophilic surface layer and a hydrophobic porous substrate that hinders membrane fouling,[73] (ii) omniphobic MD membranes that are resistant to membrane wetting,[78] and (iii) Janus membranes constructed by a superhydrophilic surface layer and an omniphobic substrate that can resist both membrane fouling and wetting.[79] In addition to robustness, future development of MD membranes should focus on reducing membrane cost and enhancing the sustainability of membrane fabrication.

In summary, numerous advanced materials have been proposed in the past few years for use in thermal desalination (*e.g.*, STD and MD). Despite recent advances in our fundamental understanding of materials properties, novel materials offer little opportunity to enhance the energy efficiency of thermal desalination. With the SE in thermal desalination defined as the latent heat of evaporation normalized by GOR (*i.e.*, SE = *L*/GOR),[9] the key to enhance energy efficiency of thermal desalination (*i.e.*, reducing SE) is to implement measures for latent heat recovery (*i.e.*, increasing GOR). Improved latent heat recovery can be realized by rational system design (*e.g.*, MSF, MED, and MD) rather than material development. Therefore, future material development for thermal desalination should target improving the robustness of the materials while simultaneously reducing their cost.

Electro-driven desalination: capacitive deionization

Obviating the need for high pressures or temperatures, electro-driven desalination is a theoretically promising alternative to RO and thermal-driven processes. Capacitive deionization (CDI), though first demonstrated in 1960 and yet to see effective commercial applications, has recently become the principally investigated electro-driven technology for desalination.[10,80–83] In CDI, a small electrical potential (<1.5 V) is applied between a pair of porous carbon or battery electrodes. The potential difference generates an electric field which drives the ions out of solution towards the oppositely charged electrodes, deionizing the water. In the case of carbon electrodes, ions are immobilized in the electrical double layers (EDLs) of the electrode micropores, whereas with battery electrodes, ions intercalate into the lattice structure.[84–86] Upon short circuiting or reversing the polarity of the electrodes, the ions are released back into solution, creating a brine stream.

In the past decade, CDI has attracted considerable research attention under the premise of being energetically favorable for brackish water desalination compared to conventional technologies, including RO.[10,82,87] Though some research has been directed towards operation modes, cell architectures, and energy recovery, the overwhelming majority of efforts have focused on the development of novel electrode materials.[84,86,87] With the electrodes being the key component of the CDI technology, material properties of electrodes are expected to largely influence the overall performance. Specifically, an ideal CDI electrode should possess high electrical conductivity and large salt adsorption capacity (SAC), while also being capable of rapid rates of adsorption and desorption. A myriad of studies aimed at enhancing these properties has culminated in three broad categories of materials: traditional carbon, advanced carbon, and pseudocapacitive. Traditional carbon materials encompass activated carbon, activated carbon cloth, carbon aerogel, and mesoporous carbon electrodes,[13,88–91] whereas we classify advanced carbon electrodes as those which incorporate graphene, carbon nanotubes, or other carbon-based nanomaterials.[92–94] Pseudocapacitive electrode materials are defined by their use of ion intercalation as a method for ion removal—either as the sole mechanism or in conjunction with EDL-based ion capture.[86,95–99]

The CDI field has commonly used charge efficiency (moles of salt removed per moles of electrical charge supplied), salt adsorption capacity, and average salt adsorption rate (ASAR) as the primary metrics for assessing the performance of electrode materials.[10] However, these parameters are limited to the evaluation of CDI, and therefore are unsuitable for comparison with other technologies. The thermodynamic energy efficiency, in contrast, is a metric which is appropriate for any desalination method, allowing for the performance of CDI to be placed in context with other technologies.[100,101] Nonetheless, very few studies have reported the thermodynamic energy efficiency of CDI, thus propagating the notion that CDI, with improved electrode materials, can become an energy efficient desalination technology.

Here, we have synthesized data for feed salinity, water recovery, salt removal, and current/voltage response over time from various studies to calculate the energy efficiency of CDI. The determined energy efficiencies are presented against the corresponding thermodynamic minimum specific energy of separation in Fig. 4a, with each assessed material classified by its type (traditional carbon, advanced carbon, or pseudocapacitive). Notably, the maximum energy efficiency achieved by any material is below 10%, while most materials show performance below even 1% energy efficiency. A recent modeling study comparing the energetic performance of CDI and RO determined a similar range of energy efficiencies for CDI, while also revealing that the energy efficiency of RO is nearly an order of magnitude greater than CDI for most separations.[100,102] A critical insight gained from the data presented in Fig. 4a is that the category of electrode material has no clear impact on the overall thermodynamic energy efficiency. In fact, the energy efficiency of traditional carbon materials even tends to be higher than most advanced carbon or pseudocapacitive materials according to the literature data collected, contradicting the notion that development of novel materials substantially improves the energetic performance of CDI.

CDI materials research has primarily focused on augmenting the electrode's specific capacitance. Increasing the specific capacitance allows for the use of more compact electrodes to achieve a given separation and extends the upper limit for practically treatable feed salinities. Larger electrode capacitance also provides the advantage of requiring a lower applied voltage to store a specific amount of charge. Specifically, this is the result of decreasing the potential drop of the Stern layer—one of several potential losses which govern the overall cell potential and theoretical energy consumption of

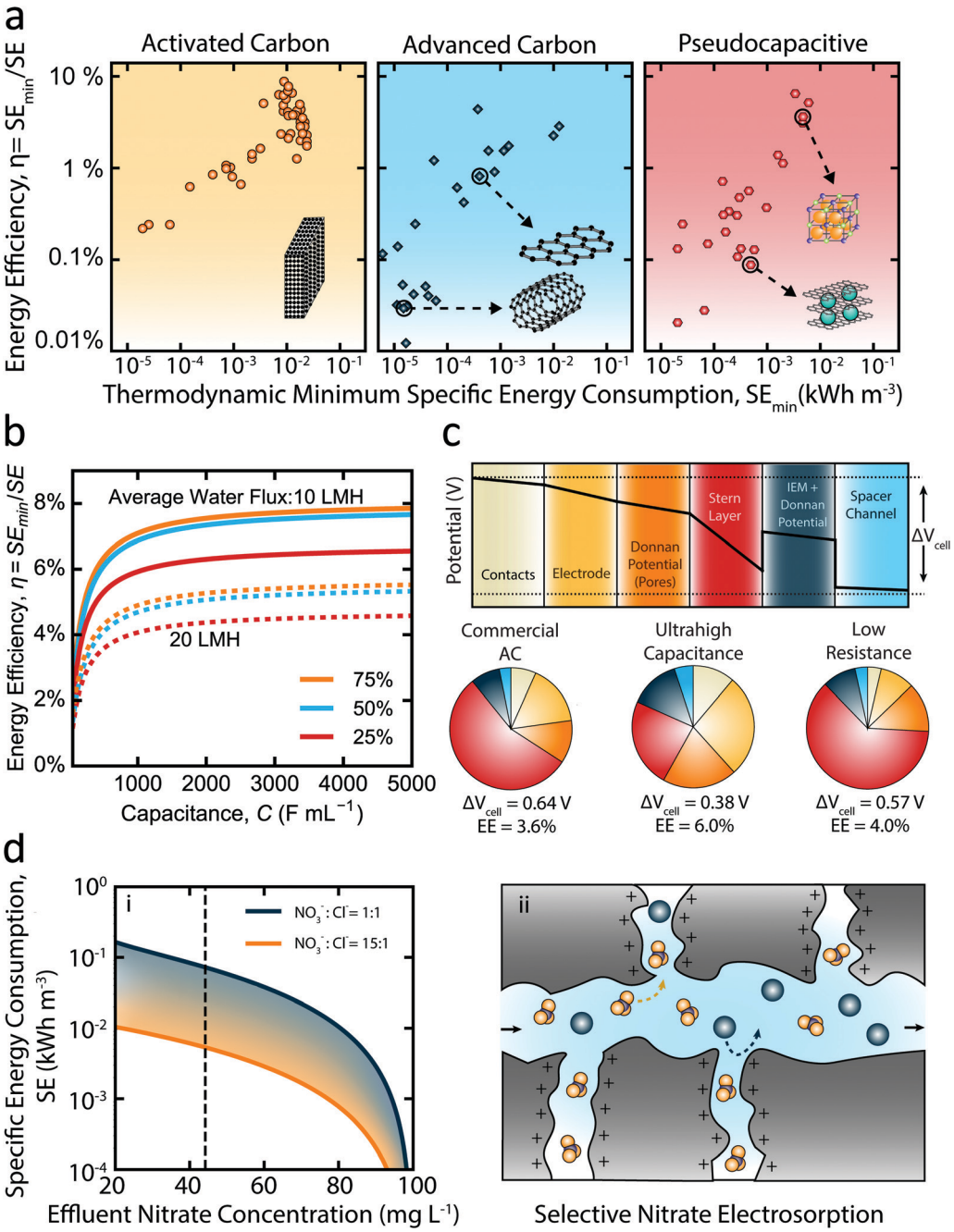

Fig. 4 The effect of enhanced capacitance, resistance, and ion–ion selectivity on the energy consumption of electrosorption. (a) Energy efficiency of capacitive deionization (CDI) *versus* the thermodynamic minimum specific energy of separation. The data is collected from the literature for (i) activated carbon materials, (ii) advanced carbon materials, and (iii) pseudocapacitive materials. The specific conditions for each data point are listed in Table S1 (ESI†). (b) Modeled energy efficiency of CDI over a range of capacitance values for salt rejections of 25% (red curves), 50% (blue curves), and 75% (orange curves). The feed salinity is 2000 mg L^{-1} and the water recovery is 50%. The solid and dashed lines represent average water fluxes of 10 L m^{-2} h^{-1} and 20 L m^{-2} h^{-1}, respectively. Additional modeling parameters used are provided in the ESI.† (c) The contribution of each potential drop to the average total cell potential (ΔV_{cell}) for three materials: commercial activated carbon, theoretical ultra-high capacitance EDL material, and theoretical low resistance EDL material. The potential drop profile shown is for commercial activated carbon and the colors displayed correspond to those used in the charts. The data shown is for 50% salt rejection and 50% water recovery of a 2000 mg L^{-1} salinity feedwater. The average water flux is fixed at 10 L m^{-2} h^{-1}. (d) Selective removal of nitrate using electrosorption. (i) The specific energy consumption of producing varying levels of nitrate effluent concentration for a feedwater composition of 500 mg L^{-1} sodium chloride and 100 mg L^{-1} nitrate. The blue and orange lines represent $NO_3^-:Cl^-$ selectivity ratios of 1 and 15, respectively. The dashed vertical line corresponds to the US EPA maximum contaminant level of nitrate in drinking water of 45 mg L^{-1} (or 10 mg L^{-1} as N). (ii) Schematic of selective nitrate electrosorption. Nitrate (orange polyatomic molecules) and chloride (blue spheres) migrate through the macropores. The nitrate molecules are preferentially immobilized in the EDLs of the micropores.

EDL-based electrosorption. The dimensionless Stern layer potential, $\Delta\phi_{st}$, can be determined according to modified-Donnan theory as

$$\Delta\phi_{st} = -\frac{\sigma_{mi} F}{C_{st} V_T} \quad (3)$$

where σ_{mi} is the volumetric charge density in the micropores, F is the Faraday constant, C_{st} is the volumetric Stern layer capacitance (the electrode specific capacitance), and V_T is the thermal voltage (where $V_T = R_g T/F$ and R_g is the ideal gas constant and T is the absolute temperature).

Though increasing the electrode capacitance reduces the Stern layer potential, it is essential to note that the capability to enhance the thermodynamic energy efficiency of CDI through increasing capacitance is severely limited. This phenomenon is demonstrated by Fig. 4b which shows the simulated energy efficiency of constant-current mode CDI over a wide range of capacitance values for a feed salinity of 2000 mg L^{-1}, salt removals of 25%, 50%, and 75% (shown by different colored lines), and average water fluxes of 10 L m^{-2} h^{-1} (dashed lines) and 20 L m^{-2} h^{-1} (solid lines). Importantly, the thermodynamic energy efficiency remains below 10% for even impractically large capacitances as high as 5000 F mL^{-1}. At low capacitance values, the Stern layer potential drop is the primary driver of energy consumption; thereby, energy efficiency initially improves with increasing capacitance. However, as capacitance is increased above ~1000 F mL^{-1}, asymptotic behavior is apparent. Above such high capacitances, further reduction of the Stern layer potential becomes negligible with respect to the contribution of the remaining potential losses, which then dictate the energetic performance.

In order to further assess the energy efficiency of CDI, we break down the average cell potential (ΔV_{cell}) over a charging cycle into its individual potential drops in Fig. 4c. Three types of electrode materials—commercial activated carbon (AC), theoretical ultra-high capacitance, and theoretical low resistance—are evaluated under typical brackish water desalination conditions. We highlight that increasing the capacitance of activated carbon electrodes (~120 F mL^{-1}) to an ultra-high capacitance material (~460 F mL^{-1}) results in only a small increase in energy efficiency (from 3.5% to 6.0%), as would be expected from our results shown in Fig. 4b. Although the Stern layer potential is significantly reduced from the increase in capacitance, the remainder of potential losses remain, which contribute significant irreversible energy losses over the charging stage. We also investigate the scenario in which the electrode conductivity is significantly enhanced from that of commercial activated carbon—as is true of many advanced carbon materials—by reducing both the electrode and contact resistances by a factor of two. Notably, we find the impact of such substantial reductions in resistance to have a negligible impact on the average cell potential and energy efficiency (Fig. 4c). Thereby, we conclude that even with optimal electrode materials the thermodynamic energy efficiency of CDI is limited to values significantly lower than RO and electrodialysis (ED), in agreement with the energy efficiency analyses performed by recent studies.[12,103]

Due to the distinct mechanism of ion removal in pseudocapacitive materials,[104] simulations of such materials are not performed. However, it is important to note that although pseudocapacitive materials allow operation at lower potentials and possess exceptional salt adsorption capacities in comparison to activated carbon, they typically suffer from very low electrical conductivity.[105,106] The high electrical resistances of pseudocapacitive materials would require operation at low current densities to avoid significant irreversible losses, resulting in stunted rates of water production. Hence, regardless of the large salt adsorption capacities of pseudocapacitive materials, mass transfer limitations of ion intercalation and large electronic resistances are likely to limit their practically achievable energy efficiency in a similar manner to EDL-based materials (Fig. 4b). This is further demonstrated by the failure of pseudocapacitive materials to demonstrate any significant advantage in energy efficiency over activated carbon or advanced carbon materials thus far (Fig. 4a). Though a particular pseudocapacitive configuration (not shown in Fig. 4a) has demonstrated higher energy efficiency, it must be noted that impractically low, near-zero productivities were required.[107] A recent study similarly found the energy efficiency of intercalation and carbon based materials to be comparable, while also demonstrating significant loss in the energetic performance of pseudocapacitive materials with increase in productivity.[108]

Given the low thermodynamic energy efficiency of CDI for water desalination applications—regardless of material improvements—we emphasize the need to shift the focus of CDI research to more appropriate applications such as the selective electrosorption of target contaminants. The energy consumption of CDI is directly related to the extent of deionization; hence, for separations which require only the removal of a particular species present in relatively low concentration, selective electrosorption may be viable. The required energy consumption of a selective electrosorption process would strongly depend on the degree of ion–ion selectivity that can be achieved. We highlight this concept by taking nitrate as a model contaminant in groundwater. In Fig. 4di we present the simulated energy consumption of reducing nitrate concentrations from 100 mg L^{-1} (in water with 500 mg L^{-1} salinity as NaCl) using varying degree of nitrate to chloride selectivity. Achieving a nitrate concentration of 45 mg L^{-1}—the US Environmental Protection Agency drinking water maximum contaminant level—consumes over an order of magnitude less energy in the case of highly selective nitrate electrosorption (*i.e.*, 15 : 1 selectivity) compared to nonselective electrosorption (*i.e.*, 1 : 1 selectivity). Though such high ion–ion selectivity has yet to be demonstrated in CDI, this analysis broadly shows the potential of selective electrosorption. In Fig. 4dii we show an illustration of selective nitrate electrosorption in the EDLs of the electrode micropores. With selective electrosorption being a nascent research area, the underlying mechanism for achieving ion–ion selectivity is not depicted. Rather, we envision novel approaches and materials which exploit the unique electrochemical and physicochemical properties of ions to be developed in the coming years.

Through our analysis we demonstrated poor energy efficiency of CDI for desalination, and—contrary to ongoing research interest—showed little potential for improvement regardless of the innovation of advanced materials. We emphasize that the development of electrodes with capacitances much greater than

traditional carbon materials offer limited benefit in terms of energy efficiency. Similarly, reduced electrode resistance is capable of only marginal enhancement in energy efficiency. Intercalation materials, though theoretically promising, are expected to suffer from similar limitations as EDL-based materials. Due to the inherent severe energetic limitations of the CDI technology, we strongly recommend the redirection of CDI research towards selective electrosorption of target ionic contaminants.

Critical need for system design

System design plays a critical role in optimizing the performance of desalination processes. Through the rational selection of process configuration and operating conditions, effective system design can reduce the driving force required to achieve the desired water production while increasing energy recovery and driving down energy consumption.[4,109] Process intensification efforts typically combine (i) staging and recycling to modulate the pressure, temperature, or electrical potential gradients driving mass transport with (ii) maximizing the recovery of mechanical, thermal, and electric energy using turbines, heat exchangers, and other energy recovery devices. In addition, system-level design plays a key role in identifying performance bottlenecks and, ultimately, the optimal performance of a given desalination process.[19,110,111] This section outlines how enhanced system design can increase the performance of pressure-, thermal-, and electro-driven desalination processes.

Pressure-driven desalination

In reverse osmosis (RO), the saline feed stream is pressurized using a high-pressure pump before being passed into the membrane module. Inside the membrane module, water permeates from the pressurized feed stream through a solute-rejecting membrane, yielding a depressurized pure permeate stream and a pressurized saline brine stream. Energy consumption in RO is primarily driven by the depressurization of water as (i) feedwater passes through the membrane into the permeate stream and (ii) the brine stream is depressurized through a series of valves before being discharged.[14,111–114] Consequently, efforts to reduce the energy consumption focus on minimizing the hydraulic pressure required to achieve a specified water flux and maximizing recovery of mechanical energy from the brine stream prior to discharge.[112,115] The transmembrane hydraulic pressure (ΔP) required in RO also depends on the target water recovery or average water flux and the final osmotic pressure of the brine (π_B). The latter is given by $\pi_B = \pi_F/(1 - \mathrm{wr})$, where π_F is the osmotic pressure of the feed and wr is the module-scale water recovery ratio of the RO stage. Concentration polarization (CP), which is caused by the buildup of rejected solutes near the feed-side membrane–solution interface, increases the osmotic pressure on the feed side of the membrane, increasing the ΔP required.[116]

Previously, improvements in membrane permeability, primarily driven by the transition from cellulose acetate to thin-film composite polyamide membranes, have driven substantial reductions in the specific energy consumption (SE) of seawater RO (SWRO). However, as demonstrated in Fig. 2b, further increasing membrane permeability will not yield significant reductions in SE. With current SWRO consuming 25% more energy than the practical minimum energy consumption of a single-RO stage ($\sim$1.6 kW h m^{-3} for a 35 g L^{-1} NaCl feed with a water recovery of 50%),[4,19] there are more opportunities to reduce the energy of desalination *via* system design.

Development and use of staged, batch, and semi-batch RO processes can yield significant SE savings of over 25%, depending on the salinity of the feedwater.[14,117] In staged processes, the brine from each stage is further pressurized before being passed to the next, with the first and intermediate stages operating at a lower hydraulic pressure than that required by a single-stage process.[118] In batch and semi-batch processes, the brine stream is recycled into the feed stream and the applied hydraulic pressure is increased with time as the feed concentration increases.[14,113,115] Staged, batch, and semi-batch processes lower the module-scale water recovery (wr) required to achieve a given system-scale recovery (WR), thereby lowering the average overpressure and thus reducing the ΔP required.[14,119,120]

The continued development of high efficiency energy recovery devices (ERDs), such as turbines or isobaric pressure exchangers, is also essential to minimize the energy lost during brine depressurization.[46] Novel pressure exchanger designs have been able to achieve energy recoveries of around 95%, though these are typically limited to prespecified isobaric operating conditions. Consequently, the development of more robust and less parameter-sensitive pressure exchangers would greatly expand the use of high efficiency ERDs.

In addition to improving its energy efficiency, system-level design should also seek to increase the maximum brine salinities that can be desalinated or concentrated by RO. Future research in this area should drive the development of high-salinity RO-based processes in addition to enabling high-pressure RO (HPRO). While RO is significantly more efficient than thermal, phase-change-based desalination technologies such as multi-effect-distillation, its application to the desalination of high salinity brines (typically 70 000 ppm and above) is limited by the high hydraulic pressures required.[6,121,122] Novel high-salinity RO-based process designs, such as osmotically assisted RO[123–125] and low salt rejection RO,[126] have the potential to reduce the hydraulic pressure required to achieve high brine salinities, expanding the applicability of RO to minimal- and zero-liquid discharge processes.[127–129] Further work is required to overcome key challenges, including internal concentration polarization and optimal membrane spacer design, that have thus far limited the practical realization of processes in which both sides of the membrane are in contact with saline streams.

Thermal-driven desalination

The implementation of latent heat recovery is the key to improving the energy efficiency of solar thermal desalination (STD). STD systems with effective latent heat recovery can be developed by connecting an external solar thermal heater to existing thermal phase-change based desalination technologies. Such technologies include multi-effect-distillation (MED), multi-stage flash (MSF), and membrane distillation (MD). In an STD system, the evaporation of water from the feed stream and its condensation into the product is accompanied by substantial

heat transfer. Effective thermal desalination technologies recover a large portion of the heat transferred to the product and reuse it to evaporate more feed water. While the mature MED and MSF technologies readily incorporate heat recovery by using condensation in one stage to drive evaporation in a subsequent stage, future design of the MD process must focus on maximizing heat recovery.

Previous studies have shown that the energy efficiency of direct contact MD (DCMD) systems can be considerably enhanced by using an external heat exchanger.[67,68] With a heat exchanger, the feed stream can be preheated by the latent heat of water condensation in the permeate stream. Some MD system configurations, such as air-gap MD (AGMD), incorporate heat recovery into the membrane module using the condensation of permeate water to directly preheat the feed stream, eliminating the need of an external heat exchanger.[130] By connecting these DCMD or AGMD systems with an external solar thermal collector, which further heats the feed stream to the required operating temperature, STD systems with effective latent heat recovery can be readily developed.

Recently, the development of novel materials has driven interest in STD systems based on solar-driven surface heating DCMD. However, as previously discussed, challenges associated with recovering the latent heat in practical surface heated systems makes such material development obsolete. Hence, to enhance the energy efficiency of MD-based STD systems, rational system design must involve MD processes with increased latent heat recovery. For example, permeate-gap MD (PGMD) and conductive-gap MD (CGMD), were recently proposed as novel process designs, which, like AGMD, incorporate heat recovery along the membrane module, but with higher energy efficiency.[131,132] We expect that further system design and optimization can guide the development of PGMD and CGMD based STD systems with effective heat recovery.

We note, however, that even STD systems with highly efficient heat recovery cannot compete with photovoltaic driven reverse osmosis (PV-RO) systems with regard to energy efficiency.[9] The most prominent advantage of STD over PV-RO is the relatively inexpensive materials required compared to photovoltaic panels and high-pressure pump and pressure vessels. Consequently, future system design of STD systems should focus on minimizing costs in addition to improving energy efficiency.

Electro-driven desalination

In capacitive deionization (CDI), an applied electric potential induces the transport of ions out of solution and into the electrical double layers or host matrix (intercalation materials) of the oppositely charged electrodes, where they are retained until discharging. Though several cell architectures and the incorporation of ion-exchange membranes (MCDI) have been investigated to enhance the performance of CDI, the underlying principle of deionization and the drivers of energy consumption remain the same amongst all designs—the transport of ions through solution and membranes (in the case of MCDI) followed by electrosorption at the electrodes.[10] Thereby, rather than assess the advantages of particular system designs, we focus the remainder of our analysis on the fundamental mechanisms of the electrosorption process which limit its energy efficiency.

A feature of CDI which has perpetuated the notion of the process being energy efficient is the ability to theoretically recover the energy utilized in the charging step. However, it is critical to note that complete recovery of the input energy is impossible. During the charging step of CDI, irreversible energy losses from parasitic side reactions, ion transport resistances (in the spacer channel and electrodes), and electronic resistances (electrode matrix, membranes, current collector, contacts) are inevitable, allowing for only a fraction of the supplied energy to be stored for potential recovery.[101] In the discharging stage, similar losses prevent complete recovery of the energy that is stored. Though decreasing the extent of salt removal and current density can reduce the magnitude of irreversible losses—allowing for a greater portion of energy to be recovered—achieving a near ideal reversible CDI process would necessitate infinitely long cycle times.[101] This effect has been shown by a previous study which required operation at small current densities, low salt removals ($<20\%$), and impractically long charge–discharge times (in the range of hours) to obtain a maximum of 79% energy recovery.[133] Hence, the salt removal and production rate of water is severely limited when high energy recoveries are desired. Under more practical operating conditions, energy recoveries below 50% are typical.[133–136] Such analysis highlights an important tradeoff of CDI by which the amount of "excess" energy that must be supplied increases with desalination rate and depth. In essence, this demonstrates that the CDI process is inherently energy inefficient for applications requiring high throughput and salt removal.[100]

The key to improving the energy efficiency of electro-driven desalination is minimizing the sources and magnitude of resistive losses. While CDI incurs multiple irreversible losses due to the need for both ion transport and electrosorption, electrodialysis (ED)—an alternate electro-driven deionization technology—relies solely on ion transport as the mechanism for salt removal, limiting the potential for excessive losses. In ED, cations and anions are selectively transported through alternating cation- and anion-exchange membranes, respectively, generating diluate and concentrate solutions.[137] Whereas CDI inherently requires the use of electrodes for electrosorption, ED employs the use of numerous membrane pairs between a single pair of electrodes, essentially eliminating the energetic contribution of the electrodes.[137,138] Recent developments in spacer channel design and ion-exchange membranes limit the overpotential required in ED,[138] making it a theoretically energy efficient technology. In a recent study, we systematically compared the energy efficiency of ED and MCDI for brackish water desalination and confirmed that the energy consumption of ED is significantly lower than MCDI—in many cases by nearly an order of magnitude. Furthermore, we demonstrated that even with substantial reduction in energetic losses and complete energy recovery, MCDI is unable to achieve the energy efficiencies of ED.[103]

Outlook

Research efforts aimed at enhancing the energy efficiency of desalination technologies have increasingly assumed a materials-based approach. In this study, we presented a systematic analysis

of RO, STD, and CDI, revealing the universal insignificance of novel materials in further enhancing the energy efficiency of pressure-, thermal-, and electro-driven desalination. Specifically, we demonstrated that ongoing efforts aimed at improving RO membrane permeability, STD solar absorptivity, and CDI electrode capacitance result in negligible reduction of specific energy consumption. Rather, we identified several system-design-based approaches which comparatively offer significant opportunity in augmenting energy efficiency of desalination technologies. Hence, we highlight the importance of process engineering—in place of innovation of advanced materials—for the sustained optimization of desalination energy efficiency.

Though ineffective for improving energy efficiency, the development of novel materials remains essential for the advancement of several important aspects of desalination performance. Despite the impressive performance of polyamide thin-film composite RO membranes, novel materials with superior water–salt selectivity could eliminate the need for additional passes or post-treatment steps,[19] thereby reducing the cost of desalination. State-of-the art polyamide TFC membranes are also highly susceptible to damage by oxidizing and disinfecting agents such as chlorine.[4] Chlorine is needed for preventing membrane biofouling—the Achilles Heel of RO desalination—in order to ensure the reliability of the RO process. Advanced membrane materials with increased chlorine tolerance could facilitate direct chlorination, thereby minimizing the required pretreatment of feedwater and chemical cleaning of fouled membranes. Hence, significant cost savings and enhanced process reliability could be realized in seawater and wastewater desalination. Additionally, in order to displace current reliance on energy intensive thermal processes, RO membranes with reinforced mechanical robustness are required to tolerate the extreme pressures encountered during the treatment of hypersaline waters. With MD, focus should be placed on ensuring process reliability through the development of membrane materials which reduce fouling and wetting propensity. Furthermore, novel materials which enable high degrees of ion–ion selectivity could extend desalination technologies to additional applications. For example, ion-selective electrosorption could potentially be applied for the selective removal of nitrate from polluted groundwaters, or the recovery of valuable resources such as lithium from seawater.

It is important to note that the energy consumption of desalination—despite being intensively investigated—is not always of primary significance. The specific energy consumption for desalination is highly dependent on the feed salinity and extent of salt removal; thus, it is the dominant factor only for the treatment of moderate to high salinity waters, such as highly brackish water, seawater, or hypersaline wastewaters. In the treatment of low salinity brackish water (salinity ranging from ~ 1 g L^{-1} to ~ 3 g L^{-1}), the energy consumption is not as substantial, and other practical considerations – such as cost, ease of operation, and process reliability—could offset the choice of a perhaps more energy efficient technology. For instance, despite the specific energy consumption of ED and RO being comparable for the desalination of low salinity feedwaters,[12,100,103] RO's contribution to brackish water desalination capacity exceeds ED by nearly 15-fold.[2] The dominance of RO over ED in brackish water desalination may largely be attributed to the considerably lower cost of polyamide TFC membranes with respect to ion-exchange membranes. Such an example highlights that desalination research priorities should be technology and source-water specific.

Overall, existing desalination technologies have attained relatively high levels of maturity and are already capable of addressing many global challenges. RO, in particular, is a reliable and highly energy efficient technology, with state-of-the-art systems operating near the theoretical practical minimum energy requirements. Hence, it is unlikely that new desalination methods will emerge to displace RO, and further improvements in the energy efficiency of desalination are expected to be incremental. Thus, we suggest future research should increasingly be directed towards enabling mature desalination technologies to operate more reliably and over a broader range of applications. Critical areas which require development are the prevention of fouling and inorganic scaling, and the reduction of waste stream volumes through higher water recoveries. Such advancements will allow for the reliable application of desalination technologies to a wide range of source waters, including industrial wastewaters, with reduced cost and minimal use of chemicals.

Conflicts of interest

There are no conflicts to declare.

Acknowledgements

This work was supported by the NSF Nanosystems Engineering Research Center for Nanotechnology-Enabled Water Treatment (EEC-1449500).

References

1 M. M. Mekonnen and A. Y. Hoekstra, *Sci. Adv.*, 2016, **2**, e1500323.
2 E. Jones, M. Qadir, M. T. H. van Vliet, V. Smakhtin and S. M. Kang, *Sci. Total Environ*, 2019, **657**, 1343–1356.
3 T. Mezher, H. Fath, Z. Abbas and A. Khaled, *Desalination*, 2011, **266**, 263–273.
4 M. Elimelech and W. A. Phillip, *Science*, 2011, **333**, 712–717.
5 D. L. Gin and R. D. Noble, *Science*, 2011, **332**, 674–676.
6 D. M. Davenport, A. Deshmukh, J. R. Werber and M. Elimelech, *Environ. Sci. Technol. Lett.*, 2018, **5**, 467–475.
7 A. Alkhudhiri, N. Darwish and N. Hilal, *Desalination*, 2012, **287**, 2–18.
8 J. Koschikowski, M. Wieghaus and M. Rommel, *Desalination*, 2003, **156**, 295–304.
9 Z. X. Wang, T. Horseman, A. P. Straub, N. Y. Yip, D. Y. Li, M. Elimelech and S. H. Lin, *Sci. Adv.*, 2019, **5**, eaax0763.
10 M. E. Suss, S. Porada, X. Sun, P. M. Biesheuvel, J. Yoon and V. Presser, *Energy Environ. Sci.*, 2015, **8**, 2296–2319.
11 J. Landon, X. Gao, A. Omosebi and K. L. Liu, *Curr. Opin. Chem. Eng.*, 2019, **25**, 1–8.
12 S. H. Lin, *Environ. Sci. Technol.*, 2020, **54**, 76–84.

13 A. Hemmatifar, A. Ramachandran, K. Liu, D. I. Oyarzun, M. Z. Bazant and J. G. Santiago, *Environ. Sci. Technol.*, 2018, **52**, 10196–10204.
14 J. R. Werber, A. Deshmukh and M. Elimelech, *Desalination*, 2017, **402**, 109–122.
15 L. Zhou, Y. L. Tan, J. Y. Wang, W. C. Xu, Y. Yuan, W. S. Cai, S. N. Zhu and J. Zhu, *Nat. Photonics*, 2016, **10**, 393.
16 L. Zhou, Y. L. Tan, D. X. Ji, B. Zhu, P. Zhang, J. Xu, Q. Q. Gan, Z. F. Yu and J. Zhu, *Sci. Adv.*, 2016, **2**, e1501227.
17 K. X. Tang, T. Z. X. Hong, L. M. You and K. Zhou, *J. Mater. Chem. A*, 2019, **7**, 26693–26743.
18 G. M. Geise, D. R. Paul and B. D. Freeman, *Prog. Polym. Sci.*, 2014, **39**, 1–42.
19 J. R. Werber, A. Deshmukh and M. Elimelech, *Environ. Sci. Technol. Lett.*, 2016, **3**, 112–120.
20 J. R. Werber, C. O. Osuji and M. Elimelech, *Nat. Rev. Mater.*, 2016, **1**, 1–15.
21 D. Cohen-Tanugi and J. C. Grossman, *Nano Lett.*, 2012, **12**, 3602–3608.
22 B. X. Mi, *Science*, 2014, **343**, 740–742.
23 B. Corry, *Energy Environ. Sci.*, 2011, **4**, 751–759.
24 S. Faucher, N. Auru, M. Z. Bazant, D. Blankschtein, A. H. Brozena, J. Cumings, J. P. de Souza, M. Elimelech, R. Epsztein, J. T. Fourkas, A. G. Rajan, H. J. Kulik, A. Levy, A. Majumdar, C. Martin, M. McEldrew, R. P. Misra, A. Noy, T. A. Pham, M. Reed, E. Schwegler, Z. Siwy, Y. H. Wang and M. Strano, *J. Phys. Chem. C*, 2019, **123**, 21309–21326.
25 D. M. Huang, C. Sendner, D. Horinek, R. R. Netz and L. Bocquet, *Phys. Rev. Lett.*, 2008, **101**, 226101.
26 S. Gravelle, L. Joly, F. Detcheverry, C. Ybert, C. Cottin-Bizonne and L. Bocquet, *Proc. Natl. Acad. Sci. U. S. A.*, 2013, **110**, 16367–16372.
27 J. K. Holt, H. G. Park, Y. M. Wang, M. Stadermann, A. B. Artyukhin, C. P. Grigoropoulos, A. Noy and O. Bakajin, *Science*, 2006, **312**, 1034–1037.
28 B. Radha, A. Esfandiar, F. C. Wang, A. P. Rooney, K. Gopinadhan, A. Keerthi, A. Mishchenko, A. Janardanan, P. Blake, L. Fumagalli, M. Lozada-Hidalgo, S. Garaj, S. J. Haigh, I. V. Grigorieva, H. A. Wu and A. K. Geim, *Nature*, 2016, **538**, 222.
29 C. L. Ritt, J. R. Werber, A. Deshmukh and M. Elimelech, *Environ. Sci. Technol.*, 2019, **53**, 6214–6224.
30 D. Cohen-Tanugi, R. K. McGovern, S. H. Dave, J. H. Lienhard and J. C. Grossman, *Energy Environ. Sci.*, 2014, **7**, 1134–1141.
31 L. F. Song and M. Elimelech, *J. Colloid Interface Sci.*, 1995, **173**, 165–180.
32 A. Seidel and M. Elimelech, *J. Membr. Sci.*, 2002, **203**, 245–255.
33 B. Sauvet-Goichon, *Desalination*, 2007, **203**, 75–81.
34 D. L. Shaffer, N. Y. Yip, J. Gilron and M. Elimelech, *J. Membr. Sci.*, 2012, **415**, 1–8.
35 B. Corry, *J. Phys. Chem. B*, 2008, **112**, 1427–1434.
36 A. K. Giri, F. Teixeira and M. N. D. S. Cordeiro, *Desalination*, 2019, **460**, 1–14.
37 E. Licsandru, I. Kocsis, Y. X. Shen, S. Murail, Y. M. Legrand, A. van der Lee, D. Tsai, M. Baaden, M. Kumar and M. Barboiu, *J. Am. Chem. Soc.*, 2016, **138**, 5403–5409.
38 J. Abraham, K. S. Vasu, C. D. Williams, K. Gopinadhan, Y. Su, C. T. Cherian, J. Dix, E. Prestat, S. J. Haigh, I. V. Grigorieva, P. Carbone, A. K. Geim and R. R. Nair, *Nat. Nanotechnol.*, 2017, **12**, 546–550.
39 S. P. Surwade, S. N. Smirnov, I. V. Vlassiouk, R. R. Unocic, G. M. Veith, S. Dai and S. M. Mahurin, *Nat. Nanotechnol.*, 2015, **10**, 459–464.
40 R. H. Tunuguntla, R. Y. Henley, Y. C. Yao, T. A. Pham, M. Wanunu and A. Noy, *Science*, 2017, **357**, 792–796.
41 J. R. Werber and M. Elimelech, *Sci. Adv.*, 2018, **4**, eaar8266.
42 L. Prozorovska and P. R. Kidambi, *Adv. Mater.*, 2018, **30**, 1801179.
43 M. S. Mauter and M. Elimelech, *Environ. Sci. Technol.*, 2008, **42**, 5843–5859.
44 C. Fritzmann, J. Lowenberg, T. Wintgens and T. Melin, *Desalination*, 2007, **216**, 1–76.
45 N. R. Warner, C. A. Christie, R. B. Jackson and A. Vengosh, *Environ. Sci. Technol.*, 2013, **47**, 11849–11857.
46 L. F. Greenlee, D. F. Lawler, B. D. Freeman, B. Marrot and P. Moulin, *Water Res.*, 2009, **43**, 2317–2348.
47 N. Ghaffour, J. Bundschuh, H. Mahmoudi and M. F. A. Goosen, *Desalination*, 2015, **356**, 94–114.
48 P. Wang, *Environ. Sci.: Nano*, 2018, **5**, 1078–1089.
49 P. Tao, G. Ni, C. Y. Song, W. Shang, J. B. Wu, J. Zhu, G. Chen and T. Deng, *Nat. Energy*, 2018, **3**, 1031–1041.
50 P. D. Dongare, A. Alabastri, S. Pedersen, K. R. Zodrow, N. J. Hogan, O. Neumann, J. J. Wu, T. X. Wang, A. Deshmukh, M. Elimelech, Q. L. Li, P. Nordlander and N. J. Halas, *Proc. Natl. Acad. Sci. U. S. A.*, 2017, **114**, 6936–6941.
51 A. Politano, P. Argurio, G. Di Profio, V. Sanna, A. Cupolillo, S. Chakraborty, H. A. Arafat and E. Curcio, *Adv. Mater.*, 2017, **29**, 1603504.
52 Y. J. Li, T. T. Gao, Z. Yang, C. J. Chen, W. Luo, J. W. Song, E. Hitz, C. Jia, Y. B. Zhou, B. Y. Liu, B. Yang and L. B. Hu, *Adv. Mater.*, 2017, **29**, 1700981.
53 G. Ni, S. H. Zandavi, S. M. Javid, S. V. Boriskina, T. Cooper and G. Chen, *Energy Environ. Sci.*, 2018, **11**, 1510–1519.
54 E. Chiavazzo, M. Morciano, F. Viglino, M. Fasano and P. Asinari, *Nat. Sustain.*, 2018, **1**, 763–772.
55 K. Bae, G. Kang, S. K. Cho, W. Park, K. Kim and W. J. Padilla, *Nat. Commun.*, 2015, **6**, 1–9.
56 M. M. Ye, J. Jia, Z. J. Wu, C. X. Qian, R. Chen, P. G. O'Brien, W. Sun, Y. C. Dong and G. A. Ozin, *Adv. Energy Mater.*, 2017, **7**, 1601811.
57 G. Ni, G. Li, S. V. Boriskina, H. X. Li, W. L. Yang, T. J. Zhang and G. Chen, *Nat. Energy*, 2016, **1**, 1–7.
58 R. L. McGinnis and M. Elimelech, *Desalination*, 2007, **207**, 370–382.
59 X. Y. Yin, Y. Zhang, Q. Q. Guo, X. B. Cai, J. F. Xiao, Z. F. Ding and J. Yang, *ACS Appl. Mater. Interfaces*, 2018, **10**, 10998–11007.
60 K. Kim, S. Yu, C. An, S. W. Kim and J. H. Jang, *ACS Appl. Mater. Interfaces*, 2018, **10**, 15602–15608.
61 M. Al-Shammiri and M. Safar, *Desalination*, 1999, **126**, 45–59.
62 H. Sayyaadi and A. Saffari, *Appl. Energy*, 2010, **87**, 1122–1133.
63 H. Sharon and K. S. Reddy, *Renewable Sustainable Energy Rev.*, 2015, **41**, 1080–1118.

64 P. Palenzuela, G. Zaragoza and D. C. Alarcon-Padilla, *Energy*, 2015, **82**, 986–995.
65 A. Deshmukh, C. Boo, V. Karanikola, S. H. Lin, A. P. Straub, T. Z. Tong, D. M. Warsinger and M. Elimelech, *Energy Environ. Sci.*, 2018, **11**, 1177–1196.
66 M. N. A. Hawlader, S. M. A. Rahman and K. A. Jahangeer, *Energy Convers. Manage.*, 2008, **49**, 1612–1619.
67 A. Deshmukh and M. Elimelech, *J. Membr. Sci.*, 2017, **539**, 458–474.
68 S. H. Lin, N. Y. Yip and M. Elimelech, *J. Membr. Sci.*, 2014, **453**, 498–515.
69 A. V. Dudchenko, C. Chen, A. Cardenas, J. Rolf and D. Jassby, *Nat. Nanotechnol.*, 2017, **12**, 557.
70 J. J. Wu, K. R. Zodrow, P. B. Szemraj and Q. L. Li, *J. Mater. Chem. A*, 2017, **5**, 23712–23719.
71 Z. X. Wang and S. H. Lin, *Water Res.*, 2017, **112**, 38–47.
72 S. Srisurichan, R. Jiraratananon and A. G. Fane, *Desalination*, 2005, **174**, 63–72.
73 Z. X. Wang, D. Y. Hou and S. H. Lin, *Environ. Sci. Technol.*, 2016, **50**, 3866–3874.
74 Z. X. Wang, Y. M. L. Chen and S. H. Lin, *J. Membr. Sci.*, 2018, **564**, 275–288.
75 M. Rezaei, D. M. Warsinger, J. H. Lienhard, M. C. Duke, T. Matsuura and W. M. Samhaber, *Water Res.*, 2018, **139**, 329–352.
76 Z. X. Wang, Y. M. L. Chen, X. M. Sun, R. Duddu and S. H. Lin, *J. Membr. Sci.*, 2018, **559**, 183–195.
77 Z. X. Wang, M. Elimelech and S. H. Lin, *Environ. Sci. Technol.*, 2016, **50**, 2132–2150.
78 S. H. Lin, S. Nejati, C. Boo, Y. X. Hu, C. O. Osuji and M. Ehmelech, *Environ. Sci. Technol. Lett.*, 2014, **1**, 443–447.
79 Y. X. Huang, Z. X. Wang, J. Jin and S. H. Lin, *Environ. Sci. Technol.*, 2017, **51**, 13304–13310.
80 B. B. Arnold and G. W. Murphy, *J. Phys. Chem.*, 1961, **65**, 135–138.
81 G. Murphy and D. Caudle, *Electrochim. Acta*, 1967, **12**, 1655–1664.
82 S. Porada, R. Zhao, A. Van Der Wal, V. Presser and P. M. Biesheuvel, *Prog. Mater. Sci.*, 2013, **58**, 1388–1442.
83 J. W. Blair and G. W. Murphy, *Saline Water Conversion*, American Chemical Society, 1960, ch. 20, vol. 27, pp. 206–223.
84 Y. Liu, C. Nie, X. Liu, X. Xu, Z. Sun and L. Pan, *RSC Adv.*, 2015, **5**, 15205–15225.
85 Y. Oren, *Desalination*, 2008, **228**, 10–29.
86 K. Singh, S. Porada, H. De Gier, P. Biesheuvel and L. De Smet, *Desalination*, 2019, **455**, 115–134.
87 F. A. AlMarzooqi, A. A. Al Ghaferi, I. Saadat and N. Hilal, *Desalination*, 2014, **342**, 3–15.
88 C. Kim, P. Srimuk, J. Lee, S. Fleischmann, M. Aslan and V. Presser, *Carbon*, 2017, **122**, 329–335.
89 Z.-H. Huang, Z. Yang, F. Kang and M. Inagaki, *J. Mater. Chem. A*, 2017, **5**, 470–496.
90 T.-Y. Ying, K.-L. Yang, S. Yiacoumi and C. Tsouris, *J. Colloid Interface Sci.*, 2002, **250**, 18–27.
91 G. Wang, B. Qian, Q. Dong, J. Yang, Z. Zhao and J. Qiu, *Sep. Purif. Technol.*, 2013, **103**, 216–221.
92 W. Shi, H. Li, X. Cao, Z. Y. Leong, J. Zhang, T. Chen, H. Zhang and H. Y. Yang, *Sci. Rep.*, 2016, **6**, 18966.
93 Y. Cho, K. S. Lee, S. Yang, J. Choi, H.-R. Park and D. K. Kim, *Energy Environ. Sci.*, 2017, **10**, 1746–1750.
94 Q. Dong, G. Wang, T. Wu, S. Peng and J. Qiu, *J. Colloid Interface Sci.*, 2015, **446**, 373–378.
95 C. Zhang, D. He, J. Ma, W. Tang and T. D. Waite, *Water Res.*, 2018, **128**, 314–330.
96 K. Wang, Y. Liu, Z. Ding, Y. Li, T. Lu and L. Pan, *J. Mater. Chem. A*, 2019, **7**, 12126–12133.
97 J. Lee, S. Kim, C. Kim and J. Yoon, *Energy Environ. Sci.*, 2014, **7**, 3683–3689.
98 J.-H. Lee, W.-S. Bae and J.-H. Choi, *Desalination*, 2010, **258**, 159–163.
99 W. Shi, X. Zhou, J. Li, E. R. Meshot, A. D. Taylor, S. Hu, J.-H. Kim, M. Elimelech and D. L. Plata, *Environ. Sci. Technol. Lett.*, 2018, **5**, 692–700.
100 M. Qin, A. Deshmukh, R. Epsztein, S. K. Patel, O. M. Owoseni, W. S. Walker and M. Elimelech, *Desalination*, 2019, **455**, 100–114.
101 L. Wang, J. Dykstra and S. Lin, *Environ. Sci. Technol.*, 2019, **53**, 3366–3378.
102 M. H. Qin, A. Deshmukh, R. Epsztein, S. K. Patel, O. M. Owoseni, W. S. Walker and M. Elimelech, *Desalination*, 2019, **462**, 48–55.
103 S. K. Patel, M. Qin, W. S. Walker and M. Elimelech, *Environ. Sci. Technol.*, 2020, **54**, 3663–3677.
104 K. Singh, H. J. M. Bouwmeester, L. C. P. M. de Smet, M. Z. Bazant and P. M. Biesheuvel, *Phys. Rev. Appl.*, 2018, 9.
105 K. Singh, S. Porada, H. D. de Gier, P. M. Biesheuvel and L. C. P. M. de Smet, *Desalination*, 2019, **455**, 115–134.
106 W. B. Shi, X. C. Zhou, J. Y. Li, E. R. Meshot, A. D. Taylor, S. Hu, J. H. Kim, M. Elimelech and D. L. Plata, *Environ. Sci. Technol. Lett.*, 2018, **5**, 692–700.
107 J. Lee, S. Kim and J. Yoon, *ACS Omega*, 2017, **2**, 1653–1659.
108 C. Gorski, J. Fortunato, T. Kim and B. Logan, *Abstr. Pap. Am. Chem. Soc.*, 2018, 255.
109 M. Elimelech, *J. Water Supply: Res. Technol.–AQUA*, 2006, **55**, 3–10.
110 A. Deshmukh and J. Lee, *Int. J. Heat Mass Transfer*, 2019, **140**, 1006–1022.
111 K. H. Mistry, R. K. McGovern, G. P. Thiel, E. K. Summers, S. M. Zubair and J. H. Lienhard, *Entropy*, 2011, **13**, 1829–1864.
112 J. H. Lienhard, *J. Heat Transfer*, 2019, 141.
113 D. M. Warsinger, E. W. Tow, K. G. Nayar and L. A. Maswadeh, *Water Res.*, 2016, **106**, 272–282.
114 S. Lin and M. Elimelech, *Desalination*, 2017, **401**, 42–52.
115 Q. J. Wei, R. K. McGovern and J. H. Lienhard, *Environ. Sci.: Water Res. Technol.*, 2017, **3**, 659–670.
116 C. P. Koutsou, S. G. Yiantsios and A. J. Karabelas, *J. Membr. Sci.*, 2009, **326**, 234–251.
117 S. H. Lin and M. Elimelech, *Desalination*, 2015, **366**, 9–14.
118 S. Lin and M. Elimelech, *Desalination*, 2015, **366**, 9–14.
119 M. H. Sharqawy, J. H. Lienhard and S. M. Zubair, *Int. J. Therm. Sci.*, 2011, **50**, 187–196.

120 J. Swaminathan, E. W. Tow, R. L. Stover and J. H. Lienhard, *Desalination*, 2019, **470**, 114097.
121 G. P. Thiel, E. W. Tow, L. D. Banchik, H. W. Chung and J. H. Lienhard, *Desalination*, 2015, **366**, 94–112.
122 T. Altmann, J. Robert, A. Bouma, J. Swaminathan and J. H. Lienhard, *Appl. Energy*, 2019, **252**, 113319.
123 T. V. Bartholomew, L. Mey, J. T. Arena, N. S. Siefert and M. S. Mauter, *Desalination*, 2017, **421**, 3–11.
124 X. Chen and N. Y. Yip, *Environ. Sci. Technol.*, 2018, **52**, 2242–2250.
125 C. D. Peters and N. P. Hankins, *Desalination*, 2019, **458**, 1–13.
126 Z. X. Wang, A. Deshmukh, Y. H. Du and M. Elimelech, *Water Res.*, 2020, 170.
127 K. G. Nayar, M. H. Sharqawy, L. D. Banchik and J. H. Lienhard, *Desalination*, 2016, **390**, 1–24.
128 A. T. Bouma and J. H. Lienhard, *Desalination*, 2018, **445**, 280–291.
129 T. Tong and M. Elimelech, *Environ. Sci. Technol.*, 2016, **50**, 6846–6855.
130 H. C. Duong, P. Cooper, B. Nelemans, T. Y. Cath and L. D. Nghiem, *Sep. Purif. Technol.*, 2016, **166**, 55–62.
131 J. Swaminathan, H. W. Chung, D. M. Warsinger and V. J. H. Lienhard, *Appl. Energy*, 2018, **211**, 715–734.
132 L. Gao, J. H. Zhang, S. Gray and J. D. Li, *Desalination*, 2019, **452**, 29–39.
133 P. Dlugolecki and A. van der Wal, *Environ. Sci. Technol.*, 2013, **47**, 4904–4910.
134 C. Tan, C. He, J. Fletcher and T. D. Waite, *Water Res.*, 2020, **168**, 115146.
135 S. I. Jeon, J. G. Yeo, S. Yang, J. Choi and D. K. Kim, *J. Mater. Chem. A*, 2014, **2**, 6378–6383.
136 J. Kang, T. Kim, H. Shin, J. Lee, J. I. Ha and J. Yoon, *Desalination*, 2016, **398**, 144–150.
137 H. Strathmann, *Desalination*, 2010, **264**, 268–288.
138 A. Campione, L. Gurreri, M. Ciofalo, G. Micale, A. Tamburini and A. Cipollina, *Desalination*, 2018, **434**, 121–160.
139 H. G. Choi, S. H. Yoon, M. Son, E. Celik, H. Park and H. Choi, *Desalin. Water Treat.*, 2016, **57**, 7545–7554.
140 J. N. Shen, C. C. Yu, H. M. Ruan, C. J. Gao and B. Van der Bruggen, *J. Membr. Sci.*, 2013, **442**, 18–26.
141 S. S. Madaeni, S. Zinadini and V. Vatanpour, *Sep. Purif. Technol.*, 2013, **111**, 98–107.
142 G. N. B. Barona, M. Choi and B. Jung, *J. Colloid Interface Sci.*, 2012, **386**, 189–197.
143 A. Gogoi, T. J. Konch, K. Raidongia and K. A. Reddy, *J. Membr. Sci.*, 2018, **563**, 785–793.
144 G. S. Lai, W. J. Lau, P. S. Goh, Y. H. Tan, B. C. Ng and A. F. Ismail, *Arabian J. Chem.*, 2019, **12**, 75–87.
145 M. Hu and B. X. Mi, *Environ. Sci. Technol.*, 2013, **47**, 3715–3723.
146 Y. Q. Yuan, X. L. Gao, Y. Wei, X. Y. Wang, J. Wang, Y. S. Zhang and C. J. Gao, *Desalination*, 2017, **405**, 29–39.
147 P. Z. Sun, R. Z. Ma, H. Deng, Z. G. Song, Z. Zhen, K. L. Wang, T. Sasaki, Z. P. Xu and H. W. Zhu, *Chem. Sci.*, 2016, **7**, 6988–6994.
148 Z. Wang, R. Sahadevan, C. N. Yeh, T. J. Menkhaus, J. X. Huang and H. Fong, *Nanotechnology*, 2017, **28**, 31LT02.
149 P. S. Zhong, T. S. Chung, K. Jeyaseelan and A. Armugam, *J. Membr. Sci.*, 2012, **407**, 27–33.
150 G. F. Sun, T. S. Chung, K. Jeyaseelan and A. Armugam, *Colloids Surf., B*, 2013, **102**, 466–471.
151 X. S. Li, R. Wang, C. Y. Tang, A. Vararattanavech, Y. Zhao, J. Torres and T. Fane, *Colloids Surf., B*, 2012, **94**, 333–340.
152 W. Y. Xie, F. He, B. F. Wang, T. S. Chung, K. Jeyaseelan, A. Armugam and Y. W. Tong, *J. Mater. Chem. A*, 2013, **1**, 7592–7600.
153 P. H. H. Duong, T. S. Chung, K. Jeyaseelan, A. Armugam, Z. C. Chen, J. Yang and M. H. Hong, *J. Membr. Sci.*, 2012, **409**, 34–43.
154 M. Q. Wang, Z. N. Wang, X. D. Wang, S. Z. Wang, W. D. Ding and C. J. Gao, *Environ. Sci. Technol.*, 2015, **49**, 3761–3768.
155 S. C. O'Hern, D. Jang, S. Bose, J. C. Idrobo, Y. Song, T. Laoui, J. Kong and R. Karnik, *Nano Lett.*, 2015, **15**, 3254–3260.
156 Y. Z. Qin, Y. Y. Hu, S. Koehler, L. H. Cai, J. J. Wen, X. J. Tan, W. W. L. Xu, Q. Sheng, X. Hou, J. M. Xue, M. Yu and D. Weitz, *ACS Appl. Mater. Interfaces*, 2017, **9**, 9239–9244.